Original article

Nuclear Medicine Communications

The prognostic relationship of 18F-FDG PET/CT metabolic and volumetric parameters in metastatic ALK+NSCLC

Nurşin Agüloğlu[a], Ayşegül Aksu[b], Damla S. Unat[c] and Murat Akyol[d]

Downloaded from http://journals.lww.com/nuclearmedicinecomm by BhDMf5ePHKav1zEoum1tQfN4a+kJLhEZgbsIHo4XMi0hCywCX1AWnYQp/IlQrHD3i3D0OdRyi7TvSFl4Cf3VC4/OAVpDDa8KKGKV0Ymy+78= on 03/31/2023

Objective **The aim of this study is to determine the role of metabolic and volumetric parameters obtained from 18Fluorine-Fluorodeoxyglucose PET/computed tomography (18F-FDG PET/CT) imaging on progression-free survival (PFS) and overall survival (OS) in patients with advanced nonsquamous cell lung carcinoma (NSCLC) with anaplastic lymphoma kinase (ALK) rearrangement.**

Methods **Pre and post-treatment PET/CT images of the ALK+NSCLC patients between January 2015 and July 2020 were evaluated. The highest standardized uptake value (SUVmax), metabolic tumor volume (MTV) and total lesion glycolysis (TLG) values were obtained from pre-tyrosine kinase inhibitor (TKI) basal PET/CT (PET_{pre}) and post-TKI PET/CT (PET_{post}) images. Total MTV (tMTV) and total TLG (tTLG) values were calculated by summing MTV and TLG values in all tumor foci. The change (Δ) in pSUVmax, pMTV, pTLG, tMTV and tTLG before and after treatment was calculated.The relationship of these parameters with OS and PFS was analyzed.**

Results **$tTLG_{pre}$, $tMTV_{pre}$, $pTLG_{pre}$, $pMTV_{pre}$, ΔSUVmax, ΔtMTV and ΔtTLG values were found to be associated with OS; ΔtMTV, ΔtTLG, $tTLG_{pre}$, $tMTV_{pre}$, $pTLG_{pre}$ and $pMTV_{pre}$ were associated with PFS. The cutoff values in both predicting OS and PFS were calculated as −31.6 and 391.1 for ΔtMTV and $tTLG_{pre}$, respectively. In Cox regression analysis, ΔtMTV and stage for OS and ΔtMTV and tTLGpre for PFS were obtained as prognostic factors.**

Conclusions **Metabolic and volumetric parameters, especially TLG values in the whole body before treatment and change in whole body MTV value, obtained from PET/CT may be useful in predicting prognosis and determining treatment strategies for patients with advanced ALK+NSCLC.** ***Nucl Med Commun*** **43: 1217–1224**
Copyright © 2022 Wolters Kluwer Health, Inc. All rights reserved.

Nuclear Medicine Communications 2022, **43**:1217–1224

Keywords: 18F-FDG PET/CT, ALK rearrangement, NSCLC

[a]Department of Nuclear Medicine, Dr. Suat Seren Chest Diseases and Surgery Training and Research Hospital, İzmir, [b]Department of Nuclear Medicine, Başakşehir Çam and Sakura City Hospital, İstanbul, [c]Dr. Suat Seren Chest Diseases and Surgery Training and Research Hospital İzmir, Turkey and [d]Department of Medical Oncology, Bakırçay University Medical School İzmir, Turkey

Correspondence to Nurşin Agüloğlu, MD, Department of Nuclear Medicine, Dr. Suat Seren Chest Diseases and Surgery Training and Research Hospital, İzmir, Turkey
Tel: +90 5052733341; e-mail: aguloglunursin@gmail.com

Received 13 February 2022 **Accepted** 9 September 2022

Introduction

Non-small cell lung cancer (NSCLC) is the most common lung cancer, and adenocarcinoma is the most common histopathological subtype [1]. Lung adenocarcinomas are genetically heterogeneous diseases based on molecular profile studies. Genomic profiling studies conducted in recent years have proven that lung adenocarcinomas are genetically very heterogeneous and complex [2]. Treatment options for NSCLC have improved greatly in recent years with the advancement in treatments that are targeted against mutated genes, such as epidermal growth factor receptor (EGFR), anaplastic lymphoma kinase (ALK), ROS proto-oncogene 1 (ROS-1) and v-raf murine sarcoma viral oncogene homolog B1(BRAF) [3–6]. Types with ALK rearrangement and EGFR mutation represent important subtypes of NSCLC targeted by tyrosine kinase inhibitors (TKI) [7]. ALK mutation detection is widely used clinically for NSCLC patients [8]. Rearrangement of the ALK gene creates potent oncogenic drivers in patients with NSCLC, occurring in approximately 3–7% of all cases. ALK+NSCLC has been associated with the absence of smoking, younger age and adenocarcinoma histology [9]. Before the discovery of the EML4–ALK fusion protein, conventional chemotherapy was used as the first line of therapy for all advanced or metastatic NSCLC. After the EML4–ALK discovery, crizotinib (first generation of ALK-directed therapy), a TKI targeting ALK, ROS1 and MET became the first US Food and Drug Administration-approved ALK inhibitor for NSCLC. Ceritinib was the first of the second-generation ALK inhibitors tested and was later approved after confirmation of its efficacy in both crizotinib-resistant and crizotinib-naive patients. Soon after, two other ALK inhibitors, alectinib and brigatinib were approved for ALK-positive patients who had failed prior crizotinib. While both are now approved in treatment-naive patients, alectinib has become the preferred agent. Most recently, we have started learning more about the indisputable role of lorlatinib, a highly potent, next-generation ALK/ROS1 TKI [10]. In addition, after the failure of crizotinib, second-generation and more potent ALK inhibitors were found to give better results with progression-free survival (PFS) over 8 months [11]. In addition to overcoming crizotinib resistance, these agents have also been shown to have high activity in brain

0143-3636 Copyright © 2022 Wolters Kluwer Health, Inc. All rights reserved.
DOI: 10.1097/MNM.0000000000001625

Copyright © 2022 Wolters Kluwer Health, Inc. Unauthorized reproduction of this article is prohibited.

Downloaded from http://journals.lww.com/nuclearmedicinecomm by BhDMf5ePHKav1zEoum1tQfN4a+kJLhEZgbsIH
o4XMi0hCywCX1AWnYQp/IlQrHD3i3D0OdRyi7TvSFl4Cf3VC4/OAVpDDa8KKGKV0Ymy+78= on 03/31/2023

metastases, a region that frequently recurs with crizotinib treatment [12]. Therefore, ALK rearrangement in lung cancer is considered an important biomarker for targeted molecular therapy in lung adenocarcinoma.

18F-fluorodeoxyglucose (FDG) PET/computed tomography (PET/CT) is the standard method for staging, treatment response monitoring and prognosis prediction for various tumors, including NSCLC [13,14]. The maximum standardized uptake value (SUV_{max}) is the most widely used parameter in clinical practice [15]. SUV_{max} is also used to predict the prognosis of NSCLC [16]. In addition, SUV_{max} shows a strong correlation with the pathological subtype and histological grade of lung adenocarcinoma [17]. Volumetric parameters including metabolic tumor volume (MTV) and total lesion glycolysis (TLG) are also parameters recently used to reflect disease burden and tumor aggressiveness in NSCLC [13,18]. In some studies, it has been suggested that there is a correlation between 18F-FDG uptake and ALK rearrangement in PET/CT [19,20]

Because survival outcomes of patients with adenocarcinoma with NSCLC differ, it is important to evaluate the prognostic factors of PET/CT parameters at each stage of cancer to predict outcomes and determine appropriate treatment options. The aim of this study was to evaluate the effects of the metabolic and volumetric parameters obtained in PET/CT imaging for the evaluation of staging and treatment response, on PFS and overall survival (OS) in a homogeneous patient group with advanced ALK mutationed NSCLC.

Methods

Patient selection

Patients who were diagnosed with NSCLC between January 2015 and July 2020 and had 18F-FDG PET/CT imaging for staging before treatment were retrospectively analyzed. Patients with histopathologically proven lung adenocarcinoma and ALK mutation detected by the high-quality probes for fluorescence in situ hybridisation method were identified. These patients were staged with TNM classification according to the eighth staging system recommended by the International Association for the Study of Lung Cancer (IASLC). Study inclusion criteria were defined as (1) histopathologically proven lung adenocarcinoma and presence of ALK mutation, (2) TKI treatment given, (3) 18F-FDG PET/CT imaging performed for staging purpose before TKI treatment and for treatment response evaluation at 3 months after TKI treatment, (4) having a minimum diameter of >1 cm of the primary tumor to avoid partial volume effects, (5) no treatment given before baseline 18F-FDG PET/CT examination and (6) having no other concomitant cancer diagnosis.

PET/CT protocol

Imaging was performed on the Philips Gemini TF 16-slice combined PET/CT scanner and the same scanner was used for all patients. Following a minimum of 6 h of fasting (blood glucose concentrations <150 mg/dl), 8–15 mCi 18F-FDG (2.5 MBq/kg body weight) was administered intravenously as defined in the European Nuclear Medicine Association (EANM) guidelines version 2.0 [21]. The time between intravenous injection and scans was 60 ± 5 min. The patients received no intravenous contrast agent. First CT images (140 kV, 100 mAs, 5-mm sections) and then PET images were acquired. Attenuation-corrected emission data were obtained using noncontrast enhanced data, extrapolated to 511 keV. PET images were acquired through emission scanning for 1.5 min per bed position, and a whole body scan from the skull vertex to the proximal thigh using 9- or 10-bed positions. The images were reconstructed with iterative algorithms over a 128 × 128 matrix. Row action maximum likelihood algorithm was used for image reconstruction.

Image analysis

The images of the patients were evaluated using LIFEx (LIFEx, Orsay, France) software [22]. PET/CT image of the patient in DICOM format was transferred to the software. The pattern and degree of primary mass involvement were evaluated and localized. The relevant region of the target lesion was evaluated semi-automatically by a nuclear medicine physician with 10 years of PET/CT experience using 18F-FDG PET/CT hybrid images (Fig. 1). Areas with an SUV_{max} value of 2.5 and above, which may belong to the primary tumor and its metastases, were segmented throughout the body [23]. SUV_{max}, mean SUV (SUV_{mean}), MTV, TLG values in pre-TKI basal PET/CT (PET_{pre}) and post-TKI PET/CT (PET_{post}) images were calculated automatically from VOIs obtained using the 41% SUV_{max} threshold. TLG value was obtained by multiplying MTV and SUV_{mean}. SUV_{max}, MTV and TLG values of the primary tumor were defined as $pSUVmax_{pre}$, $pMTV_{pre}$, $pTLG_{pre}$ before TKI, and $pSUV_{maxpost}$, $pMTV_{post}$, $pTLG_{post}$ after treatment. Pre-treatment total MTV (tMTV) and TLG (tTLG) values were calculated by summing MTV and TLG values in volume of interest obtained from the whole body and defined as $tMTV_{pre}$ and $tTLG_{pre}$. Post-treatment tMTV and tTLG values were similarly obtained and defined as $tMTV_{post}$ and $tTLG_{post}$ The change in each parameter after treatment was calculated using the formula $\%\Delta parameter = (Parameter_{post} - Parameter_{pre})/Parameter_{pre} \times 100$.

Statistical analysis

Statistical analyzes were conducted using the IBM SPSS Statistics software (version 22). Continuous variables were expressed as median and range, and categorical variables as numbers and percentages. Nonparametric tests were used in pairwise comparison due to limited sample size. PFS was defined as the time between the initial PET/CT examination and disease progression

Copyright © 2022 Wolters Kluwer Health, Inc. Unauthorized reproduction of this article is prohibited.

Fig. 1

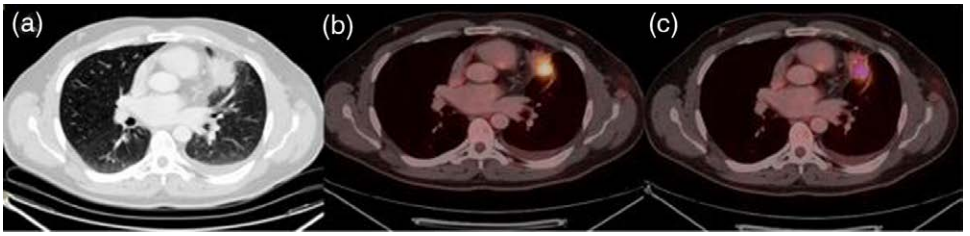

Lung lesion in the upper lobe of the left lung (a). CT image, (b). PET/CT fusion image, (c). Segmentation (with pink color) of the lung lesion in the 18F-FDG PET/CT with LIFEx software.

Downloaded from http://journals.lww.com/nuclearmedicinecomm by BhDMf5ePHKav1zEoum1tQfN4a+kJLhEZgbsIHo4XMi0hCywCX1AWnYQp/IlQrHD3i3D0OdRyi7TvSFl4Cf3VC4/OAVpDDa8KKGKV0Ymy+78= on 03/31/2023

or death, whichever occurred first. OS was calculated as the time between the initial PET/CT examination and death or the last follow-up. PFS and OS were constructed by using the Kaplan–Meier survival analysis, and log-rank tests were carried out to evaluate differences between categorical groups. To obtain suitable cutoff points, the receiver operating characteristic (ROC) curve was used. Analysis was performed according to the Youden index while determining the most appropriate cutoff value. The Cox proportional hazards model was used to evaluate prognostic variables. For multivariate analyses, the model was constructed by using the backward stepwise procedure and included significant variables that did not show correlation with each other. Correlations of the parameters with each other were evaluated with Spearman correlation analysis. *P* value <0.05 was considered significant in all statistical analyses.

Ethical approval

Local ethics committee approval was obtained. All procedures performed in studies involving human participants were in accordance with the ethical standards of the institutional research committee and with the 1964 Helsinki Declaration and its later amendments or comparable ethical standards. All patients gave their informed consent before their inclusion in the study (Approval number:2020-KAEK-139).

Results

A total of 35 patients, 12 of whom were women (34.3%), were included in the study. The mean age of the patients was 56 ± 12 (32–75) years. Fifteen (42.9%) patients were active smokers, whereas 14 (40%) patients had no history of smoking. Of the patients, 4 (11.5%) were stage IIIB, 6 (17.1%) were stage IVA, 25 (71.4%) were stage IVB. Eleven (31.4%) of the patients had visceral organ metastases and 13 (37.1%) had bone metastases (Table 1).

The median (range) $pSUV_{maxpre}$, $pMTV_{pre}$ and $pTLG_{pre}$ values of the patients were 10.8 (2.4–41.9), 14.7 (1.4–259.2) and 65.9 (9.9–2671.7), respectively. Median $tMTV_{pre}$ and $tTLG_{pre}$ values were calculated as 230.0 (37.8–1186.6) ml and 575.8 (52.2–6581.9).

Median follow-up was 12.5 (0.6–70.9) months. Twenty-one patients died. The median survival was 12.5 months (0–28.5), while the mortality rate was 60.0% (21 patients). Progression was observed in 28 patients, and median PFS was calculated as 7.5 months.

Overall survival

$tTLG_{pre}$, $tMTV_{pre}$, $pTLG_{pre}$, $pMTV_{pre}$, ΔSUV_{max}, ΔtMTV and ΔtTLG values were found to be associated with OS (*P*: 0.001, 0.006, 0.008, 0.016, 0.017, <0.001 and 0.005, respectively). Among these variables, there was no significant correlation between ΔtMTV and $tTLG_{pre}$. Of the ROC curves, the cutoff values for ΔtMTV and $tTLG_{pre}$ were calculated as –31.6 (AUC:0.873; 0.758–0.987, 95% CI, 100% sensitivity and 61.1% specificity) and 391.1 (AUC: 0.817, 0.670–0.964, 95% CI, 94.1% sensitivity and 61.1% specificity), respectively (Fig. 2). OS was found to be lower in those with ΔtMTV less than –31.6 and $tTLG_{pre}$ above 391.1 (Table 2).

Table 1 Demographic and clinical characteristics of the patients

Age (years)	
Mean±	56 ± 12
range	32–75
Gender	
Female	12
Male	23
Smoking history	
Active smoker	15
Ex-smoker	6
Never-smoker	14
Stage	
IIIB	4
IVA	6
IVB	25
Progression (*n*)	18
Mortality (*n*)	21
New lesion on PET after treatment (*n*)	8
Visceral organ metastasis	
No	24
Yes	11
Bone metastasis	
No	22
Yes	13

Copyright © 2022 Wolters Kluwer Health, Inc. Unauthorized reproduction of this article is prohibited.

Downloaded from http://journals.lww.com/nuclearmedicinecomm by BhDMf5ePHKav1zEoum1tQfN4a+kJLhEZgbsIHo4XMi0hCywCX1AWnYQp/IlQrHD3i3D0OdRyi7TvSFl4Cf3VC4/OAVpDDa8KKGKV0Ymy+78= on 03/31/2023

Survival was found to be significantly shorter in patients with stage 4B than in other patients. There was also a significant correlation between survival and visceral organ metastasis ($P<0.001$). Survival was shorter in patients with visceral organ metastases than in patients without visceral organ metastases (Fig. 3). There was no relationship between OS and the presence of bone metastases or gender.

New lesions were detected in PET_{post} images in eight patients. Survival was found to be significantly shorter in patients with new lesions compared to other patients (*P*: 0.016).

When visceral organ metastasis, presence of new lesions in PET_{post} images, stage, $tTLG_{pre}$ and ΔtMTV parameters were evaluated by Cox regression analysis, ΔtMTV (*P*: 0.004; HR, 9.574; 2.072–44.225; 95% CI) and stage (*P*: 0.031; HR, 4.438; 1.146–17.182, 95% CI) were obtained as prognostic factors predicting OS (Table 2).

Progression free survival

ΔtMTV, ΔtTLG, $tTLG_{pre}$, $tMTV_{pre}$, $pTLG_{pre}$ and $pMTV_{pre}$ were associated with PFS ($P<0.001$, 0.002, 0.007, 0.027, 0.009 and 0.032, respectively). Among these variables, there was no significant correlation between ΔtMTV and $tTLG_{pre}$. The cutoff for ΔtMTV was −31.6 (AUC, 0.873; 0.758–0.987, 95% CI, with 94.4% sensitivity and 58.8% specificity) and 391.1 for $tTLG_{pre}$ (AUC, 0.817; 0.670–0.964, 95% CI, 88.9% sensitivity and with 52.9% specificity)(Fig. 3). PFS was found to be lower in those with ΔtMTV less than −31.6 and $tTLG_{pre}$ above 391.1 (Table 2).

PFS was shorter in patients with visceral organ metastases than in patients without visceral organ metastases (Fig. 4). Apart from this, no relationship was found between PFS and the presence of bone metastases, stage, presence of new lesions or gender.

Fig. 2

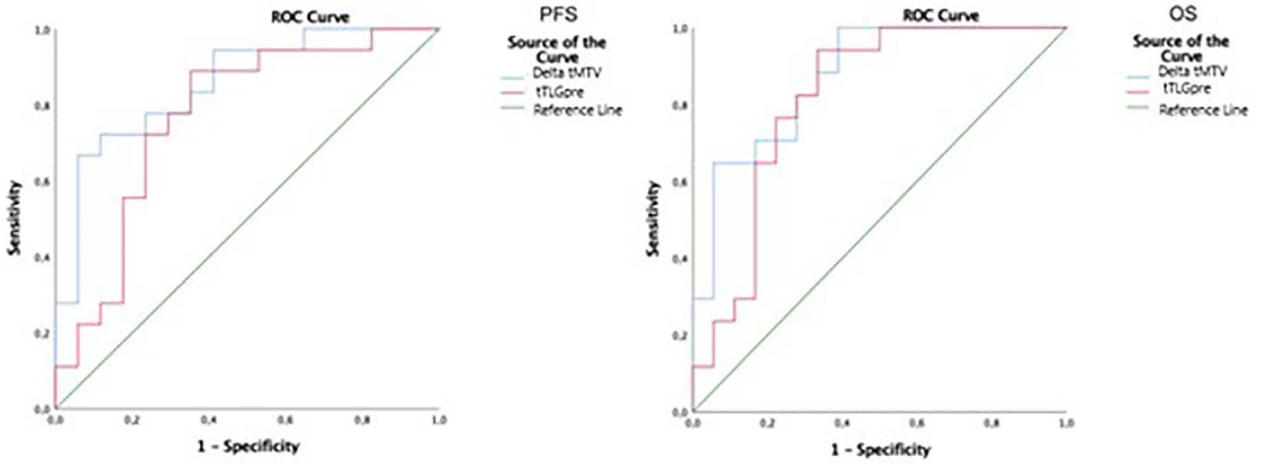

Receiver operating characteristic curves of ΔtMTV and tTLGpre parameters for overall survival and progression free survival.

Table 2 **Kaplan–Meier and Cox regression analysis results in overall survival assessment**

	Kaplan Meier		Cox regression analysis	
	Mean months (95% CI)	*P* value	*P* value	HR (95% CI)
Visceral organ metastasis				
Yes	7.4 (2.9–11.8)	<0.001	–	–
No	40.6 (27.7–53.5)			
Stage				
IIIB and IVA	52.1 (34.9–69.4)	0.013	0.031	4.438 (1.146–17.182)
IVB	21 (11.2–30.7)			
New lesion				
Yes	10.1 (2.1–18.2)	0.016	–	–
No	36.4 (24.2–48.7)			
ΔtMTV				
<−31.6	50.7 (38.9–62.4)	<0.001	0.004	9.574 (2.072–44.225)
>−31.6	19.9 (9.3–30.5)			
$tTLG_{pre}$				
<391.1	46.5 (30.6–62.5)	0.009	–	–
>391.1	20.8 (10.5–31.2)			

CI, confidence interval; HR, hazard ratio; tMTV, whole body metabolic tumor volume; tTLG, whole body total lesion glycolysis.

Copyright © 2022 Wolters Kluwer Health, Inc. Unauthorized reproduction of this article is prohibited.

Fig. 3

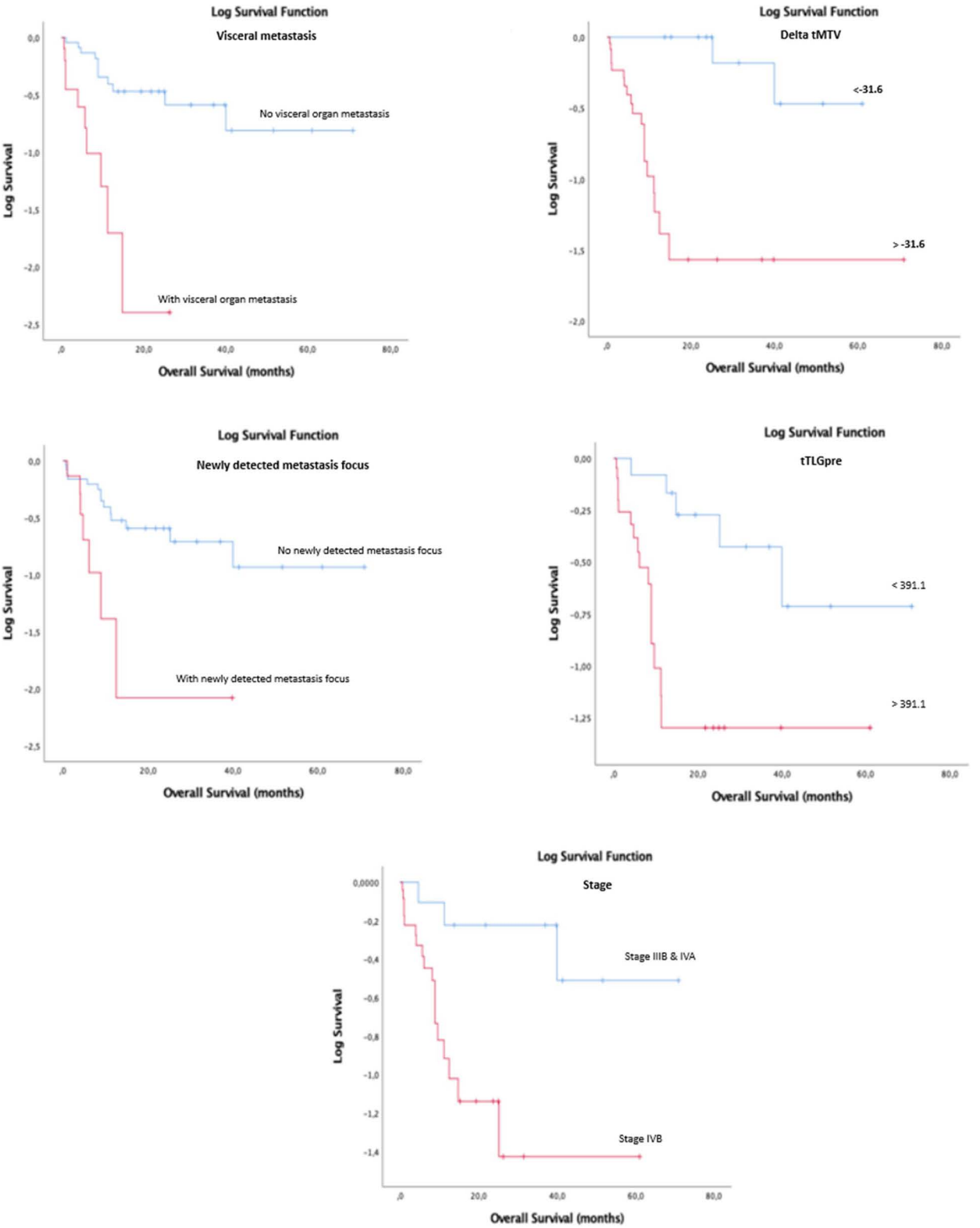

Kaplan Meier curves (log rank) of determined parameters associated with overall survival.

Downloaded from http://journals.lww.com/nuclearmedicinecomm by BhDMf5ePHKav1zEoum1tQfN4a+kJLhEZgbsIHo4XMi0hCywCX1AWnYQp/IlQrHD3i3D0OdRyi7TvSFl4Cf3VC4/OAVpDDa8KKGKV0Ymy+78= on 03/31/2023

Copyright © 2022 Wolters Kluwer Health, Inc. Unauthorized reproduction of this article is prohibited.

Fig. 4

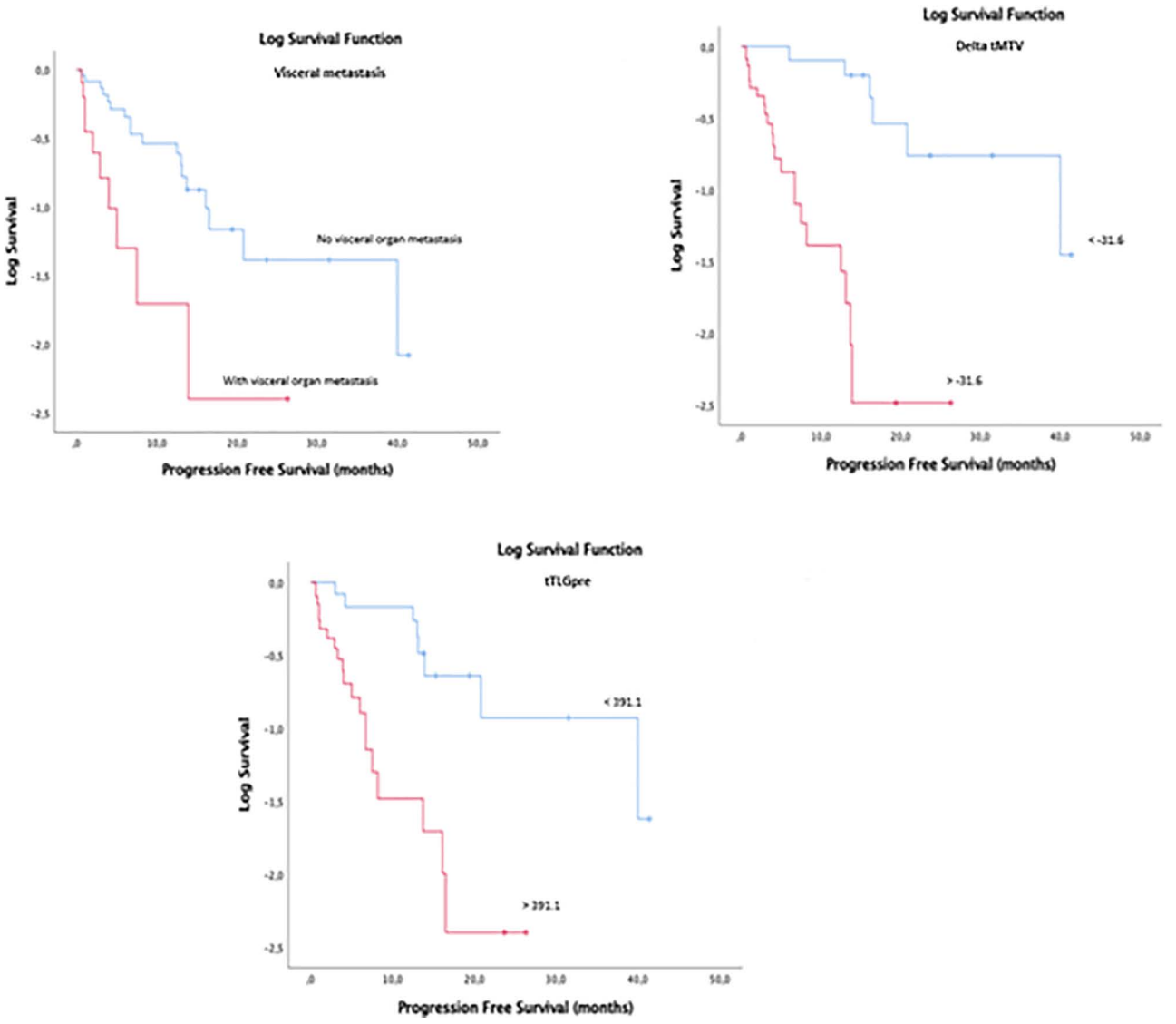

Kaplan Meier curves (log rank) of predicted parameters associated with progression free survival.

When visceral organ metastasis, $tTLG_{pre}$ and ΔtMTV parameters were evaluated by Cox regression analysis, ΔtMTV (*P*: 0.004, HR, 4.435, 1.591–12,363, 95% CI) and $tTLG_{pre}$ (*P*: 0.045; HR, 2.493; 1.021–6.089, 95 %CI) were obtained as prognostic factors predicting PFS (Table 3).

Discussion

The Application of TKIs against specific gene targets (EGFR, ALK and ROS1) has revolutionized the treatment of lung adenocarcinoma [24]. ALK inhibitors such as Crizotinib and Ceritinib are widely used to treat NSCLC patients bearing ALK mutations [25,26]. Because 18F-FDG uptake of cancer cells is associated with biological features such as proliferation, histological type, tumor differentiation and hypoxia, metabolic parameters obtained by PET/CT are important biomarkers in defining cancer heterogeneity [27,28]. Evaluation of clinical, pathological features and glucose metabolism of patients with NSCLC ALK mutation was the first step in our study. We examined the effects of metabolic and many volumetric parameters on survival with PET/CT imaging obtained after staging and treatment in an advanced stage (stage 3B, 4A and 4B) homogeneous NSCLC group bearing ALK mutation. To the best of our knowledge, this is the first study to compare many PET-based metabolic and volumetric parameters in NSCLC patients with ALK mutation. It was determined that ΔtMTV, ΔtTLG, $tTLG_{pre}$, $tMTV_{pre}$, $pTLG_{pre}$ and $pMTV_{pre}$ values were

Downloaded from http://journals.lww.com/nuclearmedicinecomm by BhDMf5ePHKav1zEoum1tQfN4a+kJLhEZgbsIHo4XMi0hCywCX1AWnYQp/IlQrHD3i3D0OdRyi7TvSFl4Cf3VC4/OAVpDDa8KKGKV0Ymy+78= on 03/31/2023

Copyright © 2022 Wolters Kluwer Health, Inc. Unauthorized reproduction of this article is prohibited.

Table 3 Kaplan Meier and Cox regression analysis results in progression-free survival assessment

	Kaplan Meier		Cox regression analysis	
	Mean months (95% CI)	*P* value	*P* value	HR (95% CI)
Visceral organ metastasis				
Yes	5.9 (1.5–10.3)	0.017	–	–
No	17.2 (11.1–23.3)			
ΔtMTV				
<–31.6	27.0 (18.5–35.5)	<0.001	0.004	4.435 (1.591–12.363)
>–31.6	7.0 (4.1–9.9)			
$tTLG_{pre}$				
<391.1	23.6 (15.1–32.1)	0.004	0.045	2.493 (1.021–6.089)
>391.1	7.3 (4.1–10.5)			

CI, confidence interval; HR, hazard ratio; tMTV, whole body metabolic tumor volume; tTLG, whole body total lesion glycolysis.

Downloaded from http://journals.lww.com/nuclearmedicinecomm by BhDMf5ePHKav1zEoum1tQfN4a+kJLhEZgbsIHo4XMi0hCywCX1AWnYQp/IlQrHD3i3D0OdRyi7TvSFl4Cf3VC4/OAVpDDa8KKGKV0Ymy+78= on 03/31/2023

associated with PFS, whereas $tTLG_{pre}$, $tMTV_{pre}$, $pTLG_{pre}$, $pMTV_{pre}$, ΔSUV_{max}, ΔtMTV and ΔtTLG values were associated with OS. $tTLG_{pre}$ was determined as the most effective prognostic factor for predicting PFS and ΔtMTV as the most effective prognostic factor for predicting both PFS and OS. In our study, high tTLG values were associated with shorter PFS, and higher ΔtMTV values were associated with shorter PFS and OS. With this result, we showed that post-treatment PET/CT may contribute to evaluating the prognosis of patients with ALK mutation. ΔtMTV values may provide an assessment of treatment response, as well as information about tumor chemosensitivity and prognosis prediction. We think that determining the group of patients with ALK mutations who can benefit from effective treatments and who can develop rapid progression after treatment may have an impact on survival.

Choi *et al.* [20] found a significantly higher SUV_{max} (10.51) in 18 patients with ALK mutation compared to NSCLC patients with different mutations. Jeong *et al.* [19] found a higher mean SUV_{max} (11.8) in 41 patients with ALK mutations compared to patients with NSCLC with different mutations. High SUV values were associated with a worse prognosis in patients with NSCLC in studies, therefore, high SUV values reflect a more aggressive tumor biology [16,29]. This result suggests that the higher glucose metabolism in the lung mass with ALK mutation is associated with more malignant features. In our study, the SUV_{max} median value was found to be similar to other studies. Glucose metabolism levels in tumor tissues measured on 18F-FDG PET/CT can assess and reflect tumor invasiveness [30,31].

Metabolic parameters of PET/CT, including SUV_{max}, MTV, and TLG, have been reported to be promising tumor prognostic indicators in NSCLC [32,33]. SUV_{max} may fail to reflect the behavior of tumor tissue [34]. While the volume-based PET/CT parameter TLG provides complementary information about tumor heterogeneity and total disease burden, MTV can provide prognostic information [33,35]. Im *et al.*'s meta-analysis, where many studies are evaluated suggests that metabolic parameters such as TLG and MTV are better predictors of treatment outcomes in lung cancer than SUV_{max} [36]. Several studies have shown that MTV and TLG volumetric parameters are superior to SUV_{max} in estimating PFS [32,37,38]. In our study, volumetric parameters obtained by basal PET/CT and total MTV and TLG parameters of all malignant lesions were found to be associated with PFS and OS, while SUV_{max} value was not associated with PFS and OS, similar to other studies.

This study has the limitation of retrospective single institution experience in a relatively small group of 35 patients with ALK mutations staged by PET/CT. The small rate of ALK rearrangement in the NSCLC adenocarcinoma patient population was an inevitable limitation for a single-center study. Larger prospective multicenter studies are required for validation.

In our study, TLG values in the whole body before treatment and change in the whole body MTV value were determined as the most effective prognostic factors for predicting PFS and both PFS and OS respectively. Primary tumor parameters (SUV_{max}, SUV_{mean}, MTV and TLG) may also provide some prognostic value. Parameters obtained from PET/CT for staging and treatment response evaluation may be useful in predicting prognosis and determining treatment strategies for patients with advanced lung adenocarcinoma with ALK mutation.

Acknowledgements

Conflicts of interest

There are no conflicts of interest.

References

1 Devarakonda S, Morgensztern D, Govindan R. Genomic alterations in lung adenocarcinoma. *Lancet Oncol.* 2015 **16**: e342–e351.
2 Kerr KM. Pulmonary adenocarcinomas: classification and reporting. *Histopathology* 2009; **54**:12–27.
3 Herbst RS, Morgensztern D, Boshoff C. The biology and management of non-small cell lung cancer. *Nature.* 2018; **553**:446–454.
4 Arbour KC, Riely GJ. Systemic therapy for locally advanced and metastatic non-small cell lung cancer: a review. *JAMA* 2019; **322**:764–774.
5 McLoughlin EM, Gentzler RD. Epidermal growth factor receptor mutations. *Thorac Surg Clin* 2020; **30**:127–136.
6 Serritella AV, Bestvina CM. Anaplastic lymphoma kinase mutation-positive non-small cell lung cancer. *Thorac Surg Clin* 2020; **30**:137–146.
7 Putora PM, Schneider T, Rodriguez R, Früh M. Targeted therapy in non-small cell lung cancer. *Breathe* 2012; **8**:206–215.

Copyright © 2022 Wolters Kluwer Health, Inc. Unauthorized reproduction of this article is prohibited.

8 Du X, Shao Y, Qin HF, Tai YH, Gao HJ. ALK-rearrangement in non-small cell lung cancer (NSCLC). *Thorac Cancer* 2018; **9**:423–430.
9 Shaw AT, Yeap BY, Mino-Kenudson M, Digumarthy SR, Costa DB, Heist RS, *et al*. Clinical features and outcome of patients with non-small-cell lung cancer who harbor EML4-ALK. *J Clin Oncol* 2009; **27**:4247–4253.
10 Kwak EL, Bang YJ, Camidge DR, Shaw AT, Solomon B, Maki RG, *et al*. Anaplastic lymphoma kinase inhibition in non-small-cell lung cancer. *N Engl J Med* 2010; **363**:1693–1703.
11 Shaw AT, Kim D-W, Mehra R, Tan DS, Felip E, Chow LQ, *et al*. Ceritinib in ALK-rearranged non-small cell lung cancer. *N Engl J Med* 2014; **370**:1189–1197.
12 Chun SG, Choe KS, Iyengar P, Yordy JS, Timmerman RD: Isolated central nervous system progression on crizotinib: an Achilles heel of non-small cell lung cancer with EML4-ALK translocation? *Cancer Biol Ther* 2012;**13**:1376–1383.
13 Moon SH, Hyun SH, Choi JY. Prognostic significance of volume-based PET parameters in cancer patients. *Korean journal of radiology: official journal of the Korean Radiological Society*. 2013;**14**:1– 12.
14 Zhu A, Lee D, Shim H. Metabolic positron emission tomography imaging in cancer detection and therapy response. *Semin Oncol* 2011; **38**:55–69.
15 Paidpally V, Chirindel A, Lam S, Agrawal N, Quon H, Subramaniam RM. FDG-PET/CT imaging biomarkers in head and neck squamous cell carcinoma. *Imaging in medicine* 2012; **4**:633–647.
16 Paesmans M, Berghmans T, Dusart M, *et al*. Primary tumor standardized uptake value measured on fluorodeoxyglucose positron emission tomography is of prognostic value for survival in non-small cell lung cancer: update of a systematic review and meta-analysis by the European Lung Cancer Working Party. *J Thorac Oncol* 2008; **3**:6–12.
17 Chao-Hua C, Yi-Chen Y, Ko-Han L, *et al*. Histological subtypes of lung adenocarcinoma have differential 18 F-fluorodeoxyglucose uptakes on the positron emission tomography/computed tomography scan. *J Thorac Oncol* 2011; **6**:1697–1703.
18 Davison J, Mercier G, Russo G, Subramaniam RM. PET-based primary tumor volumetric parameters and survival of patients with non-small cell lung carcinoma. *AJR Am J Roentgenol* 2013; **200**:635–640.
19 Jeong CJ, Lee HY, Han J, Jeong JY, Lee KS, Choi YL, Choi JY: Role of imaging biomarkers in predicting anaplastic lymphoma kinase-positive lung adenocarcinoma. *Clin Nucl Med* 2015; **40**:e34–e39.
20 Choi H, Paeng JC, Kim DW, Lee JK, Park CM, Kang KW, Chung JK, Lee DS: Metabolic and metastatic characteristics of ALK-rearranged lung adenocarcinoma on FDG PET/CT. *Lung Cancer* 2013;**79**:242–247
21 Boellaard R, Delgado-Bolton R, Oyen WJ, Giammarile F, Tatsch K, Eschner W, *et al*. FDG PET/CT: EANM procedure guidelines for tumour imaging: version 2.0. *Eur J Nucl Med Mol Imaging* 2015;**42**:328–354.
22 Nioche C, Orlhac F, Boughdad S, Reuzé S, Goya-Outi J, Robert C, Pellot-Barakat C, Soussan M, Frouin F, Buvat I. LIFEx: a freeware for radiomic feature calculation in multimodality imaging to accelerate advances in the characterization of tumor heterogeneity. *Cancer Res*. 2018;**78**:4786–4789.
23 Chenlu L, Changsheng M, Jinghao D *et al*. Using CT texture analysis to differentiate between peripheral lung cancer and pulmonary inflammatory pseudotumor. *BMC Medical Imaging* 2020; **20**:75.
24 Harada G, Gongora ABL, da Costa CM, Santini FC. TRK inhibitors in non-small cell lung cancer. *Curr Treat Options Oncol* 2020; **21**:39.
25 Shaw AT, Bauer TM, Marinis FD, Felip E, Goto Y, Liu G, *et al*. First-Line Lorlatinib or Crizotinib in Advanced *ALK*-Positive Lung Cancer. *N Engl J Med* 2020; **383**:2018–2029.
26 Elliott J, Bai Z, Hsieh SC, Kelly SE, Chen L, Skidmore B, *et al*. ALK inhibitors for non-small cell lung cancer: a systematic review and network meta-analysis. *PLoS One* 2020; **15**:e0229179.
27 Jadvar H, Alavi A, Gambhir SS. 18F-FDG uptake in lung, breast, and colon cancers: molecular biology correlates and disease characterization. *J Nucl Med* 2009; **50**:1820–1827.
28 Vesselle H, Schmidt RA, Pugsley JM, Li M, Kohlmyer SG, Vallires E, *et al*. Lung cancer proliferation correlates with [F-18]fluorodeoxyglucose uptake by positron emission tomography. *Clin Cancer Res* 2000; **6**:3837–3844.
29 Borst GR, Belderbos JS, Boellaard R, Comans EF, De Jaeger K, Lammertsma AA, *et al*. Standardised FDG uptake: a prognostic factor for inoperable non-small cell lung cancer. *Eur J Cancer* 2005; **41**:1533–1541.
30 Fu L, Alam MS, Ren Y, Guan W, Wu H, Wang Q, *et al*. Utility of Maximum standard uptake value as a predictor for differentiating the invasiveness of T1 stage pulmonary adenocarcinoma. *Clin Lung Cancer* 2018; **19**:221–229.
31 Eriguchi D, Shimada Y, Imai K, Furumoto H, Okano T, Masuno R, *et al*. Predictive accuracy of lepidic growth subtypes in early-stage adenocarcinoma of the lung by quantitative CT histogram and FDG-PET. *Lung Cancer* 2018; **125**:14–21.
32 Hyun SH, Ahn HK, Kim H, Ahn MJ, Park K, Ahn YC, *et al*. Volume-based assessment by (18)F-FDG PET/CT predicts survival in patients with stage III non-small-cell lung cancer. *Eur J Nucl Med Mol Imaging* 2014; **41**:50–58.
33 Liao S, Penney BC, Zhang H, Suzuki K, Pu Y. Prognostic value of the quantitative metabolic volumetric measurement on 18F-FDG PET/CT in stage IV nonsurgical small-cell lung cancer. *Acad Radiol* 2012; **19**:69–77.
34 Yip SS, Kim J, Coroller TP, Parmar C, Velazquez ER, Huynh E, *et al*. Associations between somatic mutations and metabolic imaging phenotypes in non-small cell lung Cancer. *J Nucl Med* 2017; **58**:569–576.
35 Chen HH, Chiu NT, Su WC, Guo HR, Lee BF. Prognostic value of whole-body total lesion glycolysis at pretreatment FDG PET/CT in non-small cell lung cancer. *Radiology* 2012; **264**:559–566.
36 Im H, Pak K, Cheon G, Kang K, Kim S, Kim I. Prognostic value of volumetric parameters of (18)F-FDG PET in non-small-cell lung cancer: a meta-analysis. *Eur J Nucl Med Mol Imaging*. 2015; **42**:241–51.
37 Lee HY, Hyun SH, Lee KS, Kim BT, Kim J, Shim YM, *et al*. Volume-based parameter of 18)F-FDG PET/CT in malignant pleural mesothelioma: prediction of therapeutic response and prognostic implications. *Ann Surg Oncol* 2010; **17**:2787–2794.
38 Yoo J, Choi JY, Lee KT, Heo JS, Park SB, Moon SH, *et al*. Prognostic significance of volume-based metabolic parameters by (18)F-FDG PET/CT in gallbladder carcinoma. *Nucl Med Mol Imaging* 2012; **46**:201–206.

Downloaded from http://journals.lww.com/nuclearmedicinecomm by BhDMf5ePHKav1zEoum1tQfN4a+kJLhEZgbsIHo4XMi0hCywCX1AWnYQp/IlQrHD3i3D0OdRyi7TvSFl4Cf3VC4/OAVpDDa8KKGKV0Ymy+78= on 03/31/2023

Copyright © 2022 Wolters Kluwer Health, Inc. Unauthorized reproduction of this article is prohibited.